International Journal of Engineering Research & Technology (IJERT)
ISSN: 2278-0181
Vol. 3 Issue 7, July - 2014

Utilization of Co-ZIF as Catalyst for Organic Transformations

[!] Adewale Olamoyesan,[!]Hua Zhang, Yu Deng, [!]Jiexiang Wang, [φ]Bodunde Joseph Owolabi, [!]Bing Hui Chen
[!] College of Chemistry and Chemical Engineering, National Engineering Laboratory for Green Chemical Productions of Alcohols–Ethers–Esters, Xiamen University, Xiamen 361005, China.
Department of Chemistry, Federal University of Technology, Akure, P.M.B 704, Ondo State, Nigeria.

***Abstract*— An excellent conversions of benzaldehyde was obtained under solvent and solvent free conditions, by utilizing $Co(im)_20.5DMA$ as catalyst for the synthesis of benzylidene malononitrile. The catalytic prospect of this crystalline porous framework was extended to oxidation reactions involving ethylene glycol (EG) and ethylbenzene (EB). Unexpectedly, EG was totally oxidized to oxalic acid; which demonstrates the catalyst non-selectivity towards glycolic acid. For EB oxidation under a solvent less condition in the presence of oxygen as oxidant (0.8 Mpa), and a 42 % conversion was achieved with 78.4 % selectivity for acetophenone at 120 °C for a period of 2 h.**

Keywords*— Metal organic frameworks, Zeolitic imidazolate frameworks, Ethylene glycol, Ethylbenzene.

I. INTRODCUTION

The next phase after the substantial foundation of Metal-organic frameworks (MOFs) synthetic chemistry is the utilization of its chemical versatility and functionality. MOFs have been identified for prospective applications in gas separation and storage, sensors, drug delivery and catalysis [1-4]. These crystalline frameworks functionalities for catalysis can arise from: metal ions, organic linkers, the pore sites, encapsulated active sites [5]. The self supporting strategy offers by this class of materials have shown to be effective in a number of different reactions with various coordination complexes [5,6,7], and also have provided a desirable environmentally benign and selective catalytic process. MOFs as other heterogeneous catalysts are advantageous for liquid phase organic transformation, as they are easily recoverable with minimal environmental impact [8].

Zeolite imidazolate frameworks (ZIFs) a sub class of this porous material; where its crystal structures share the same topologies as those that can be found in zeolites, were chose for the catalytic exploration and evaluation on the basis of its thermal and chemical stability[9]. Till date, only a few examples of the potential of ZIFs as catalysts have been recently published: ZIF-8 catalyzes the trans-esterification of vegetable oil [10]; and is an active catalyst for the Knoevenagel reaction [11]; also ZIF-9 has been used as a catalyst in the oxidation of aromatic oxygenates [12] and for C-C coupling reaction [13]; ZIF-8 catalyzes the conversion of CO_2 to chloropropene carbonate [14] and for synthesis of ethyl methyl carbonate [15] ; the most recent is Au@ZIF-8 and Au@ZIF-90 for aerobic oxidation of benzyl alcohol [16].

Indeed, in this direction we decide to explore and evaluate the catalytic prospect of Co-ZIFs for; Knoevenagel condensation of benzaldehyde with malononitrile, oxidation of ethylene glycol and ethylbenzene, where the ligand catalyses the condensation and the metal ion (Co^{2+}) for oxidation transformation of the substrates of interest.

II. EXPERIMENTAL

A. Materials

Cobalt nitrate hexahydrate (99.50%), Benzaldehyde (98.50%), Malononitrile (99.00%), Ethylene glycol (99.00%), Ethylbenzene (98.50%), N,N-dimethylacetamide (DMA) (99.50%), N,N-dimethylformamide (DMF) (99.50%), Dichloromethane (DCM) (99.50%) and Piperazine (99.00%) were purchased from Sinopharm Chemical Reagent, China . These chemicals were used without further purification.

B. Preparation of Co-ZIFs

- *Synthesis of $[Co(im)_20.5DMA]_\infty$ (1)*

$Co(im)_20.5DMA$ was synthesized based on the procedure reported by Tian *et al* [17]. $Co(NO_3)_2.6H_2O$ (3.638 g, 0.0125 mol), $C_3H_4N_2$ (1.7 g, 0.025 mol), and piperazine (1.075 g,0.0125 mol) were dissolved in DMA (65 mL).The reaction mixture was stirred at room temperature for 2 h .Then, the solution was then placed in a Teflon-lined autoclave and heated in an oven at 135 °C and maintained at 135 °C for 24 h. After unassisted cooling to room temperature, the violet crystals were collected and washed with DMA (30 mL) with a yield of ~45% based on imidazolate ligand.

- *Synthesis of $Co(im)_20.5DMF$ (2)*

$Co(NO_3)_26H_2O$ (3.64 g, 0.0125 mol) and $C_3H_4N_2$ (2.35 g,0.345 mol) were added to DMF (60 mL). The reaction mixture was stirred at room temperature for 12 h .Then, the solution was placed in a Teflon-lined autoclave and heated in an oven at 140 °C and maintained at 140 °C for 48 h. After unassisted cooling to room temperature, the violet crystals were collected and washed with DMF (30 mL) with a yield of ~25% based on imidazolate ligand.

- *Synthesis of Co(nim)$_2$ (3)*

$Co(NO_3)_2 6H_2O$ (2.183 g,7.5 mmol) and 4-nitroimidazole,$C_3H_3N_3O_2$ (8.482 g, 75 mmol) were added to DMF (30 mL). The reaction mixture was stirred at room temperature for 12 h .Then, the solution was placed in a Teflon-lined autoclave and heated in an oven and maintained at 120 °C for 24 h. After cooling to room temperature, the cube-shaped single crystals were collected and washed with DMF (30 mL).

C. Characterization of Co-ZIFs

The Single crystal data were collected on a Bruker SMART APEX CCD diffractometer with graphite monochromated Mo Kα radiation (λ = 0.71073 Å) radiation. Powder XRD patterns of the samples were recorded on a Phillips X'Pert Pro Super X-ray diffractometer equipped with X'Celerator detection system and Cu*Kα* radiation (40 kV and 30 mA) was used as the X-ray source. Scans were performed over the 2θ range from 5° to 45°, using a resolution of 0.028° in a step size of the 0.0167° and counting of 10 s per step. The morphology of the samples was observed by a field-emission scanning electron microscope (FESEM, LEO-1530, Germany) combined with energy dispersive spectroscopy (EDS) and Olympus optical microscopy. Fourier transform infrared (FT-IR) measurements were recorded on a Nicolet 740 FTIR spectrometer at ambient conditions. TG–DTA was carried out in static air using a SDT Q600 V20.9 Build 20 thermal analyzer in the temperature range 30–800 °C at a heating rate of 10 °Cmin^{-1}. The UV–vis spectra were recorded on a Shimadzu 1750 UV-vis Spectrophotometer at room temperature.

D. Catalytic activity

- *Typical procedure for the Knoevenagel condensation reaction*

Inspired by the principle of green chemistry, the initial reaction was carried out in a solvent free environment and at room temperature. The Knoevenagel reaction between benzaldehyde and malononitrile using Co(im)$_2$ 0.5DMA as catalyst was carried out in a batch wise 25 ml round-bottom flask magnetically stirred. A mixture of benzaldehyde (5.16 ml, 0.05mol), and malononitrile (3.03 g, 0.05 mol) was placed into the flask and stirred for 2 min, then (0.295 g, 5 mmol) of catalyst was added to the reaction mixture. The catalyst concentration was calculated with respect to the cobalt/benzaldehyde molar ratio. The reaction vessel was continuously stirred until the completion of the reaction, where the porous crystal solid absorbed all the solvent and formed a sticky amorphous brown gel after 5 min. After the completion of the reaction, the product was obtained with the addition of 10 ml DCM, and then the solid cobalt imidazolate framework was separated from the mixture by simple centrifugation and then followed by filtration when necessary; for reusability sake the catalyst was washed with copious amount of DCM dried under vacuum at 60 ºC for 12 h. The reaction mixture was analyzed by Shimadzu GC 2010, filtering through a short silica gel pad and then analyze by GC and the product identity was confirmed by GC-MS when necessary.

Gas chromatographic (GC) analyses were performed using a Shimadzu GC 2010 equipped with a flame ionization detector (FID) and a DB-35 column (length = 60 m, inner diameter = 0.25 mm, and film thickness = 0.25 μm). The temperature program for GC analysis was kept at 70 ºC for 6 min and heated samples from 70 to 280 ºC at 5 ºC /min and held them at 280 ºC for 15 min. Injector and detector temperatures were set constant at 280 ºC with a column flow rate of 2.0 m/L^{-1}.

- *Typical procedure for the oxidation of Ethylene Glycol*

The investigation of possible oxidation of ethylene glycol into less toxic or useful products such as glycolic acid was carried out in a 300ml Parr reactor (550 series). Ethylene glycol, NaOH (50mmol) and the catalyst (metal/ reactant = 10^{-3}) were mixed with distilled water to a total volume of 100ml. The reaction mixture was charged into the autoclave and exchanged three times with pure oxygen, and then pressurized with O_2 to 300KPa, stirred and heated to appropriate temperature. After the reaction mixture was cooled to room temperature, the excess gas was vented and the resultant liquid was taken out and the catalyst was separated from the mixture by simple filtration. The aqueous solution was analyzed by a Dionex Ultimate U3000 HPLC system, equipped with online degasser, dual gradient pump (loading pump and analytical pump), an auto sampler with a 100 μL sample loop, a column oven, and a diode array detector. The Chroméléon software (Dionex, Sunnyvale, USA) was used to control the system to collect data. A reversed phase column of Acclaim ® Polar Advantage II (PA II) C18 (150 mm×4.6 mm, 5 μm) was used with aqueous 0.01 M H_2SO_4 (0.8 ml/min) as the eluent. Samples of reaction mixture (0.1 ml) were diluted (10 ml) by using the eluent.

- *Typical procedure for the oxidation of Ethylbenzene*

The heterogeneous catalytic oxidation reaction was performed in 100 ml stainless steel reactor. Ethylbenzene (98.50%) was used as obtained without any further purification, and the asynthesized catalyst with DMA guest molecule was exchanged by dichloromethane (DCM) (3 x15 ml) for 3 days, then the residual solvents were removed under vacuum at 200 ºC for 6 h. In a typical experimental procedure, ethylbenzene (30 ml, 0.4 mol) and cobalt imidazolate framework Co(im)$_2$.0.5DMA (0.928 g, 0.04 mol) were added into the 100 ml autoclave, and exchanged three times with pure oxygen, then filled with O_2 to 0.8x10^6 Pa, stirred and heated to 120 °C for a period of 2 h. After the reaction mixture was cooled to room temperature in a bath of ice/water mixture, the excess gas was vented and the resultant liquid was taken out and the solid catalyst was separated from the mixture by simple centrifugation followed by filtration when necessary; for reusability sake the catalyst was washed with copious amount of DCM dried under vacuum at 60 ºC for 12 h.

The filtrate was analyzed with Shimadzu GC 2010, filtering through a short silica gel pad and the product identity was confirmed by GC-MS. Gas chromatographic (GC) analyses were performed using a Shimadzu GC 2010 equipped with a

flame ionization detector (FID) and a AT-SE 30 column (length = 30 m, inner diameter = 0.25 mm, and film thickness = 0.33 μm). The temperature program for GC analysis was started from 40 to 200 ºC at 10 ºC/min and kept at 200 ºC for 10 min, and then heated from 200 to 280 ºC and held them at 280 ºC for 2 min. Injector and detector temperatures were set constant at 200 ºC and 280 ºC respectively with a column flow rate 2.0 ml^{-1}.

III RESULTS AND DISCUSSION

A. Characterization of the catalysts

There exist high degrees of correspondence between the experimental and simulated XRD patterns for both $Co(im)_2$0.5DMA and $Co(im)_2$0.5DMF as shown in (Fig. 1-2); which is an indication that the bulk material is a true representation of the single crystal. On the other hands, the powder pattern of simulated $Co(nim)_2$ revealed three clearly observable peaks and several weak reflections in the range of 2Θ (12-40) degrees, which are not visible on the experimental pattern (Fig. 3). The observed difference in diffractograms could be attributed to the preferred orientation of growth during $Co(nim)_2$ synthesis. An apparent decline in the intensity of the peaks were observed for used $Co(im)_2$0.5DMA.

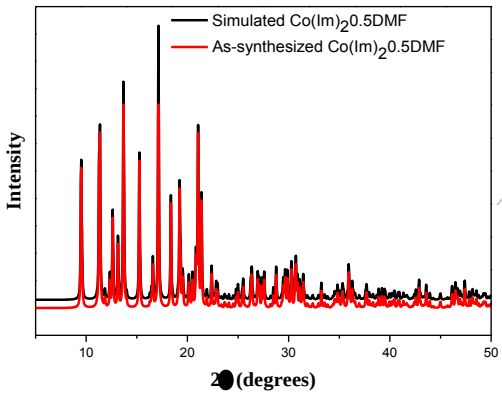

Fig. 1. Comparison of the experimental PXRD of as-synthesized

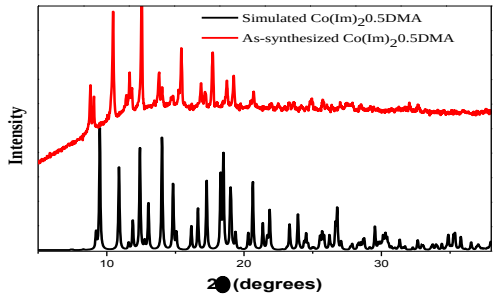

$Co(im)_2$0.5DMA with the simulated pattern from its single crystal structure.

Fig. 2. Comparison of the experimental PXRD of as-synthesized $Co(im)_2$0.5DMF with the simulated pattern from its single crystal structure.

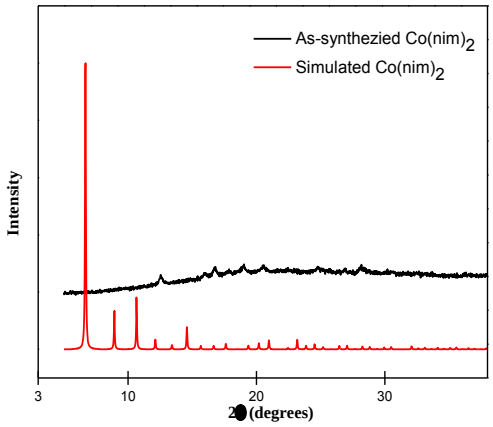

Fig. 3. Comparison of the experimental PXRD of as-synthesized $Co(nim)_2$ with the simulated pattern from its single crystal structure.

catalyst and this was most significant for Knoevenagel condensation (Fig. 4), where the crystalline material transformed to sticky amorphous. Noteworthy, the catalytic active site of this porous crystal material was retained during the course of rerun experiments, and consistent conversions were obtained for the reusability test. For $Co(nim)_2$ diffraction patterns (Fig.5), the peaks of the used catalysts were maintained as the fresh material, this demonstrate the stability of $Co(nim)_2$ after usage as catalyst for Knoevenagel condensation.

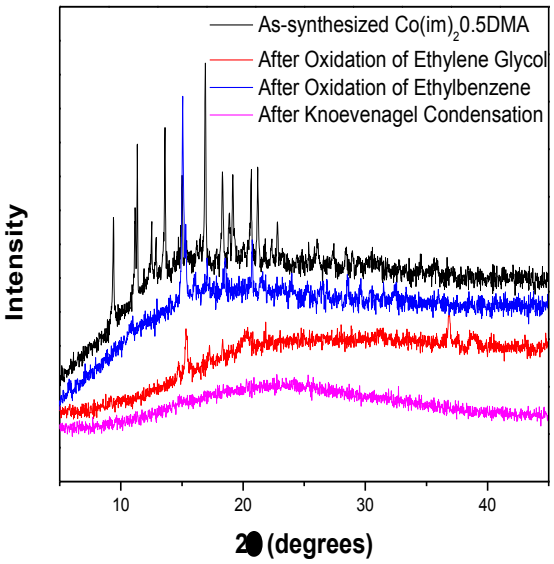

Fig. 4. Comparison of PXRD pattern of fresh $Co(im)_2$0.5DMA and after usage for specific organic synthesis reaction.

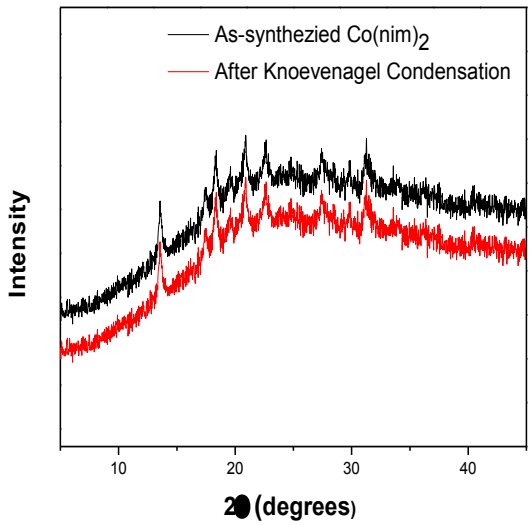

Fig. 5. Comparison of PXRD pattern of fresh $Co(nim)_2$ and after usage for specific organic synthesis reaction.

The SEM shows a highly crystalline dipyramid (Fig. 6 (a)) and rhombic prism (Fig. 6 (b)) shape crystals which confirmed the aforementioned crystal system specified by the Single Crystal X-ray analysis, with a crystal sizes ranging approximately between 100 and 200 µm. Also, the optical micrograms confirmed the shape of the crystalline frameworks (see Fig. A in Supporting Appendix) which are in agreement with previous reports on cobalt imidazolate frameworks [17, 18].

The TGA (Fig. 7) shows weight loss of 8% up to 200 ˚C corresponds to the release of guest molecules (0.5 DMA), and the most noteworthy feature in this result was found between the temperature range of 200 - 340 °C with little weight loss, indicating that the $Co(im)_2$0.5DMA was stable up to 340 °C. Afterward, a very rapid weight-loss step of 54% was observed as the temperature increased from 340 to 430°C, demonstrating the thermal decomposition of the $Co(im)_2$0.5DMA.

The FT-IR spectra of $Co(im)_2$0.5DMA along side with that of imidazole are shown in Fig. 8. The presence of strong and broad N–H--N hydrogen bond was observed in the FT-IR spectra of imidazole ranging from 3350 - 2200cm^{-1} with a maximum at about 2613cm^{-1} and associated with weak band near 1830 cm^{-1}; while the observed disappearance of these absorption bands, evidently indicates the deprotonation of the imidazole ligands during the formation of this porous crystalline framework [5]. Besides, stretching vibrations of C - H bonds was observed near 3125 cm^{-1} and the double bond in the imidazole ring absorbs at 1650 cm^{-1}. Fig. B1 in Supporting Appendix shows the FT-IR spectra of fresh $Co(im)_2$0.5DMA along with used catalyst after specific organic transformation. In addition, the spectra for nitroimidazole along with fresh and used $Co(nim)_2$ are shown in Fig. B2, similar absorption bands were observed as $Co(im)_2$0.5DMA spectra with an inclusion of NO_2 stretching vibration near 1580cm^{-1}.

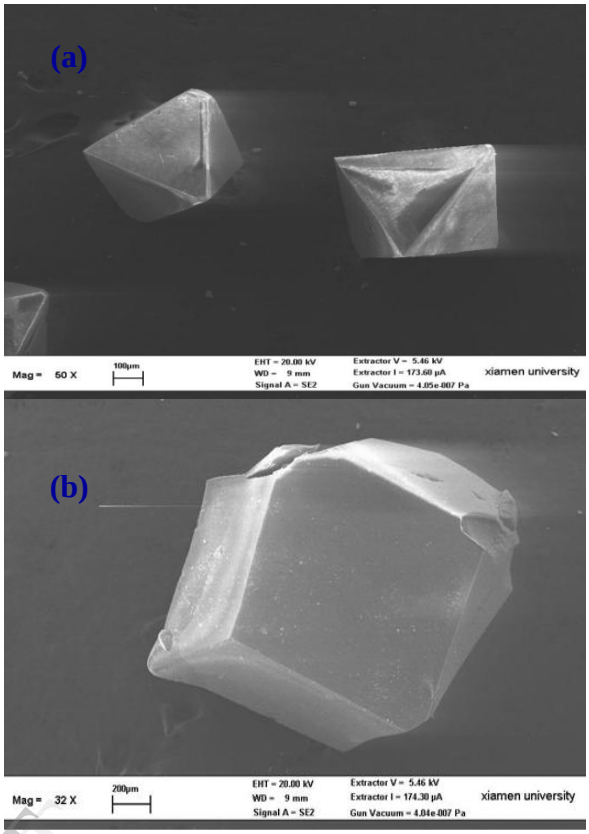

Fig. 6. SEM micrograms of (a) $Co(im)_2$0.5DMA and (b) $Co(im)_2$0.5DMF.

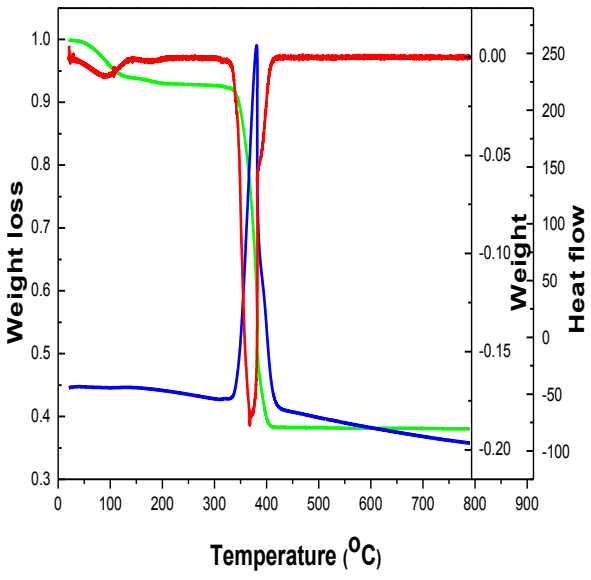

Fig. 7. TGA analysis of the $Co(im)_2$0.5DMA.

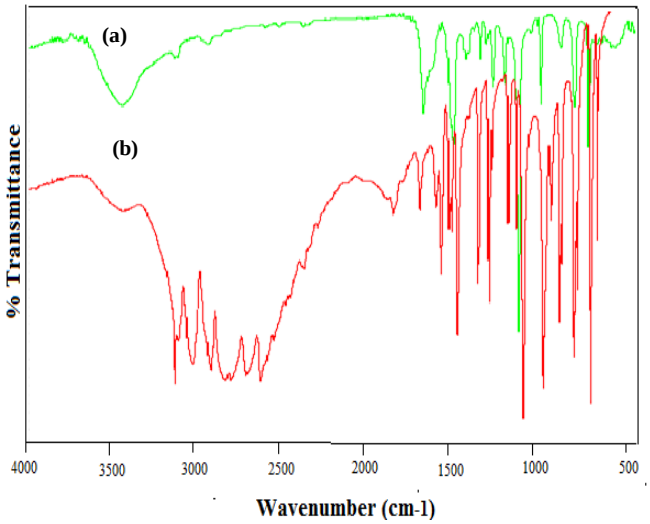

Fig.8.FT-IR spectra of (a) $Co(im)_2$.0.5DMA and (b) imidazole.

In order to compare the UV-vis spectral properties of the single crystal with that of the cobalt complex in solution, the spectra of the solution was prepared in the same manner as the solution for crystal synthesis. As shown in Fig. 9-11, the single crystal spectra do not differ very much in comparison with that of its complex solution. The UV-Vis absorption spectra of the crystalline frameworks show several similar absorption bands, the maximum absorptions of $Co(im)_2$0.5DMA (**1**), $Co(im)_2$0.5DMF (**2**) and $Co(nim)_2$ (**3**) are respectively about 600, 597 and 596 nm . These maximum can be assigned to the spin-allowed d-d transition 4A2(F) → 4 T2 (P) of tetrahedral Co(II) ions[19,20], also a weak shoulder at about 535 , 534 and 533 nm are observed respectively for the complexes. The λ max of **1**, **2** and **3** were hypsochromically shifted by about 10, 100 and 8nm, respectively when compared with their complex solution.

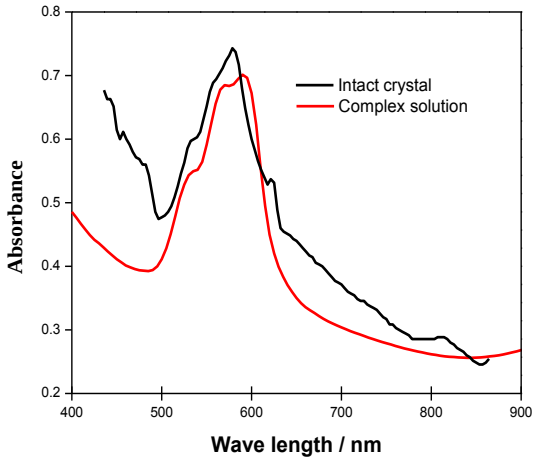

Fig.9. UV-Vis spectra of $Co(im)_2$0.5DMA and that of the complex in solution.

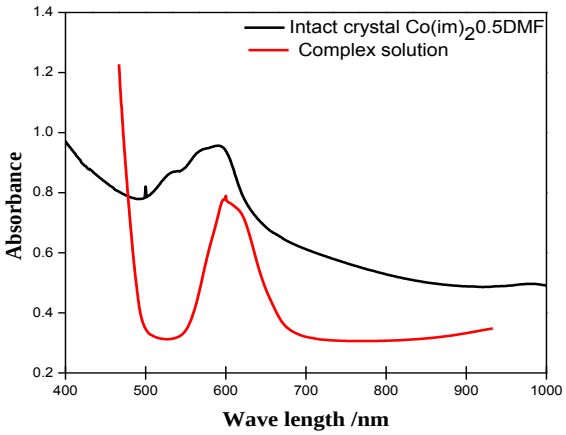

Fig. 10. UV-Vis spectra of $Co(im)_2$0.5DMF and that of the complex in solution.

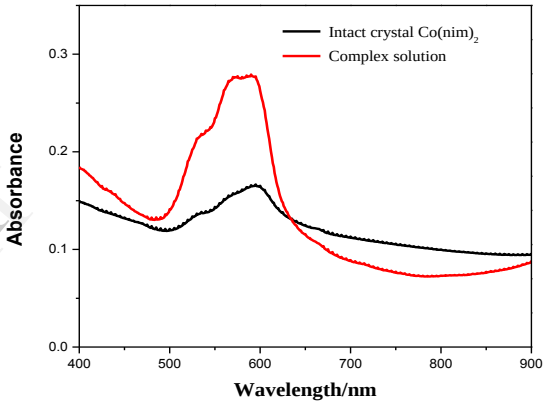

Fig. 11. UV-Vis spectra of $Co(nim)_2$ and that of the complex in solution.

B. *Catalytic activity of Co-ZIFs*

- *Knoevenagel Condensation*

$Co(im)_2$0.5DMA is accessed for its catalytic activity for Knoevenagel condensation reaction under a solvent free condition (Scheme 1). A conversion of 96% was obtained after 5 min, and the recovered catalyst was subsequently tested for reusability with an excellent conversion of 98%. Hence, while DCM was used as solvent with the same amount of reactants and catalyst; a conversion of 98% was

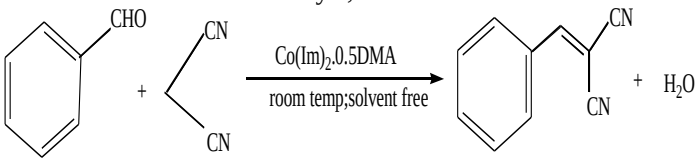

Scheme 1. Knoevenagel reaction of benzaldehyde with malononitrile using $[Co(im)_2$0.5DMA$]_\infty$ as catalyst.

achieved in 10 min without any significant change after three cycle of the catalyst (Fig. 12).

In good agreement with previous reports [11,13,21], using 5 mol % imidazole and the metal precursor ($Co(NO_3)_26H_2O$) instead of $Co(im)_20.5DMA$ a 93% and 7% of quantitative conversion was achieved after 5 min. Since, both imidazole and $Co(NO_3)_26H_2O$ can only act as homogenous catalysts, which may not be practical from green perspective. To demonstrate that the catalytic activity of $Co(im)_20.5DMA$ is devoid of any leached active species (imidazolate linkers), the reaction was carried out under solvent condition by using 5 % mol of catalyst concentration, and then the reaction was stopped after 2 min filtered and analyzed by GC , and portion of the filtrate was transferred to another vial and stirred for further 5 and 8 min respectively. During the 2 min 57% conversion was obtained, and no

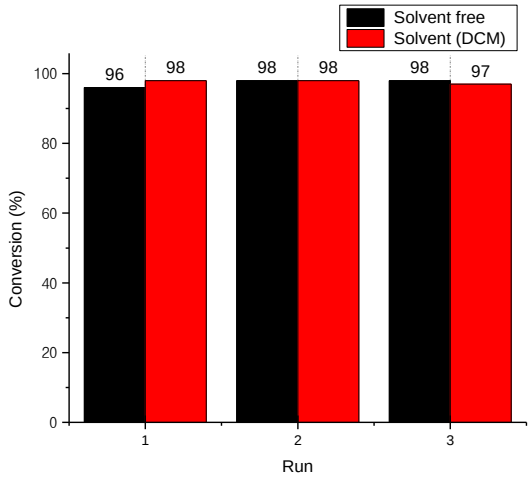

Fig. 12. Catalyst reusability studies of $Co(im)_20.5DMA$ with respect to conversion under solvent free and solvent condition.

and conversion was observed afterward while stirring further the filtrate. We then tested $Co(nim)_2$ for Knoevenagel reaction with an initial conversion of over 90% obtained for both solvent free and solvent condition that took 20 and 30 min respectively, and there was no observed loss of intrinsic catalytic activity after reusability test as shown in Fig. 13.

Consequently, the slight lower conversion obtained with $Co(nim)_2$ could be attributed to the base weakening influence of the nitro group on the imidazolate linker, however, $Co(im)_20.5DMA$is more basic with a corresponding higher conversion and shorter reaction time. The prominent active centers of Co-ZIFs are the basic sites (imidazolate linkers), with a plausible activity by Co^{2+} ions (Lewis acid sites) for Knoevenagel reaction as observed with $Co(NO_3)_2.6H_2O$ when utilized as catalyst for this reaction. Although the $Co2^+$ ions could activate the carbonyl substrates of the Knoevenagel condensation acting as catalyst or co-catalyst for the reaction [22,23]; markedly, the extra frameworks of CoO (impurities entrapped inside the pore cavities as either nanoparticles or segregated crystallites) also contribute to the catalytic activities of the CO-ZIFs [23-26]. Comparative studies of the catalytic behaviour of Co-ZIFs with other state-of-the-art catalysts for the Knoevenagel condensation are shown in Table I. We found that Co-ZIFs are efficient further reaction

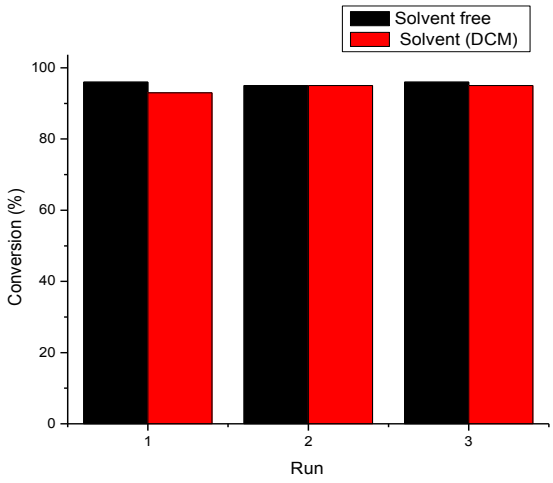

Fig. 13. Catalyst reusability studies of $Co(nim)_2$ with respect to conversion under solvent free and solvent condition.

TABLEI.COMPARATIVE STUDIES OF THE CATALYTIC BEHAVIOUR OF $CO(IM)_20.5DMA$ WITH OTHER CATALYSTS FOR KNOEVENAGEL CONDENSATION.

Catalyst	Reaction conditions	Time (min)	Conv/ Yield	Ref
Diaminosilane-functionalized cobalt spinel ferrite ($CoFe_2O_4$)	2.5 mol% of catalyst; Solvent: benzene ; and at room temp; reactants mole ratio: malononitrile/benzaldehyde 2:1	5	100	[27]
ZIF-8	5 mol % catalyst, Solvent:Toluene; and at room temp; reactants mole ratio:malononitrile/benzaldehyde 4:1	120	100	[11]
Amine-functionalized mesoporous zirconia	1.79 mol% catalyst; Methanol; reactant mole ratio: and at room temp benzaldehyde/ malonic ester1:1	1440	89	[28]
Guanidium lactate ionic liquid	2.5 mmol IL ;and at room temp; reactants mole ratio: malononitrile/benzaldehyde 1:1	2	93[a]	[29]
In/AlMCM-41	0.06 mol% of In/AlMCM-41; under reflux condition in ethanol; reactants mole ratio: malononitrile/benzaldehyde 1.2:1	25	95[a]	[30]
$Co(im)_20.5DMA$	10 mol% Catalyst; and at room temp; reactants mole ratio: malononitrile/benzaldehyde 1:1	5	98	[T]
$Co(nim)_2$	10 mol % Catalyst; and at room temp; reactants mole ratio: malononitrile/benzaldehyde 1:1	20	96	[T]

a is product yield; T *is this paper,* IL *is ionic liquid*

in the Knoevenagel condensation for the synthesis of benzylidene malononitrile. The conversions obtained with Co-ZIFs are higher than some previously reported catalysts, where higher active methylene compounds moles were required for the same reaction and longer reaction time. Conversely, our catalysts exhibited less activity in the Knoevenagel condensation as compared to some base catalysts such as functionalized cobalt spinel ferrite and amine functionalized mesoporous zirconia[11,27,28].

- *Oxidation of Ethylene Glycol*

In an effort to transform ethylene glycol to glycolic acid the catalytic prospect of this material was explored as shown in Scheme 2. The result obtained demonstrated the catalyst non-selectivity towards glycolic acid. In this case, ethylene glycol was totally oxidized to oxalic acid without any trace of glycolic acid, even when the reaction time and temperature was reduced to 30 min and 30 °C respectively (Table II). We proposed that to achieve a selective oxidation of ethylene glycol to glycolic acid, noble metal such as Au, Ag and Pt can be incorporated into the porous frameworks as metal ions or supported on it, since noble metals have been demonstrated to be effective for the selective conversion of EG to glycolic acid [31,32].

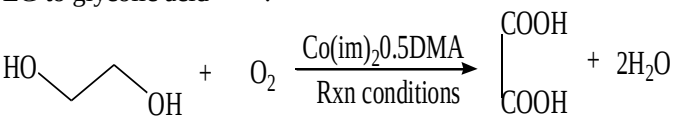

Scheme 2. Catalytic oxidation of ethylene glycol using $Co(im)_2$0.5DMA as catalyst.

TABLE II. CATALYTIC OXIDATION OF ETHYLENE GLYCOL USING CO-ZIF AS HETEROGENEOUS CATALYST.

Catalyst	Temp(°C)	Time(h)	Yield (%)
$Co(im)_2$0.5DMA	70	6	85
$Co(im)_2$0.5DMA	30	3	65
$Co(im)_2$0.5DMA	30	1[!]	17
$Co(im)_2$0.5DMA	30	0.5	6.5

! Reaction mixture with NaOH

- *Oxidation of Ethylbenzene*

In an effort to implement green principle in this chemical transformation procedure, the oxidation of ethylbenzene was carried out without using solvent and the oxidant employed was molecular oxygen. The $Co(im)_2$0.5DMA was found to be highly active and selective for the conversion of ethylbenzene to acetophenone. Hence, at temperature of 120 °C and a pressure of $0.8x10^6$pa, we observed 42% conversion of the substrate and a remarkable selectivity of 78.4% for acetophenone as shown in Scheme 3. As presented in Table III, the results for optimized reaction process for ethylbenzene oxidation are summarized. The conversion of ethylbenzene and its selectivity towards acetophenone increased rapidly from 42-71.3 %, as temperature increased from 120 – 150 °C. When the reaction time was increased from 2-10 h, initially both the conversion and selectivity of acetophonene increased

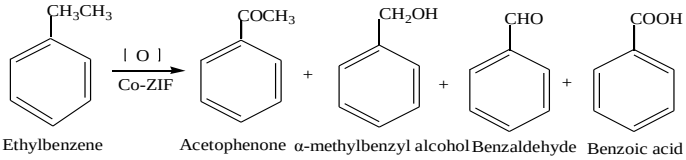

Scheme 3. Result of oxidation of ethylbenzene using $Co(im)_2$0.5DMA as catalyst

TABLE III: CATALYTIC OXIDATION OF ETHYLBENZENE UNDER SOLVENT LESS CONDITION USING CO-ZIFS AS HETEROGENEOUS CATALYST.

S/N	Reaction Conditions	Conv (%)	Selectivity (%)			
			I	II	III	IV
1	120 °C	42	78.4	15.5	0.7	5.4
2	130 °C	57.5	79.5	13.8	0.6	6.1
3	140 °C	67.8	83.6	12.1	0.7	3.6
4	150 °C	71.3	84.5	7.8	0.5	7.2
5	4 h	70.4	87.3	6.1	0.6	6.0
6	6 h	70.8	86.5	5.7	0.5	7.3
7	8 h	71.3	81.4	4.9	0.4	13.3
8	10 h	71.5	80.5	4.1	0.4	15.0
9	1.5 Mpa	60.5	85.7	6.3	0.7	7.3
10	2.0 Mpa	67.4	87.8	5.4	0.5	6.3
11	0.08 mol	54.3	83.5	4.3	1.2	11
12	0.12 mol	59.5	83.9	4.5	0.8	10.8
13	0.16 mol	65.4	86.8	3.9	0.3	9
14	0.2 mol	71.2	84.5	3.1	0.3	12.1
15	$Co(nim)_2$	40.3	78.7	15.1	0.6	5.6
16	$Co(OAC)_2.6H_20$	39.4	69.1	18.3	2.4	10.2

and afterward no obvious change was observed due to inhibition by the product, while as a result of over oxidation of acetophenone or methylbezylalcohol to benzoic acid the selectivity decreased gradually from 87.3-80.5%. As the pressure increased from 0.8-2.0 MPa, the conversion of the substrate and selectivity to acetophenone increased as well. Likewise, the effect of catalyst concentration was studied, as the concentration Co-ZIF increased from 0.04 – 0.2 mol, the conversion of substrate rapidly increased from 42-71.2% and acetophenone selectivity increased from 78.4-84.5%. Furthermore, the investigation of $Co(nim)_2$ and $Co(NO_3)_2.6H_2O$ for catalytic oxidation of substrate under similar experimental condition, it was found that the 40.3 and 39.4 % of the ethylbenzene was converted to main product respectively, and a reasonable selectivity was obtained for both the crystalline porous framework and cobalt precursor.

IV. CONCLUSION

We examined Knoevenagel condensation of benzaldehyde using Co-ZIFs as catalyst for the synthesis of benzylidene malononitrile under a solvent and solvent less condition with a remarkable conversion. The Co^{2+} of the coordination complex was explored for oxidation of ethylbenzene and ethylene glycol, since cobalt metal precursor was an important catalyst for oxidation transformation. As a result, the crystalline framework was not selective towards glycolic acid but oxidized the substrate to oxalic which is less toxic.

Moreover, Co-ZIF was found to be highly active for the oxidation of ethylbenzene and remarkably selective for acetophenone. This work accentuates the usefulness of MOFs as heterogeneous catalysts for organic synthesis, where either the metal ions or ligands can serve as catalyst for different organic transformations of interest.

ACKNOWLEDGMENT

The authors gratefully acknowledge funding and support provided by the department of Chemical and Biochemical Engineering, Xiamen University towards this research. We would also like to thank colleagues and graduate student who contributed to this work in particular Zheng Yong of Structural Chemistry for his guidance on crystal growth and Shelxtl software.

REFERENCES

[1] A.U. Czaja, N. Trukhan and U. Müller, "Industrial applications of metal organic frameworks," Chem. Soc. Rev., vol. 38, pp. 1284-1293, April 2009.

[2] B. Yilmaz, N. Trukhan and U, Müller, "Industrial outlook on zeolites and metal organic frameworks," Chin.J. Catal., vol. 33, pp.3-10, January 2012.

[3] R.J. Kuppler, D.J. Timmons, Q-R. Fang, J-R. Li, T.A. Makal, M.D. Young, D. Yuan, D. Zhao, W. Zhuang and H-C. Zhou, "Potential applications of metal-organic frameworks," Coord. Chem. Rev., vol. 253, pp. 3042–3066, December 2009.

[4] O. Shekhah, J. Liu, R.A. Fischer and Ch. Wöll, "Mof thin films:existing and future applications," Chem. Soc. Rev., vol. 40, pp. 1081-106, January 2011.

[5] A. Corma, H. Garcı´a and F.X. Llabrés i Xamena, "Engineering metal organic frameworks for heterogeneous catalysis," Chem. Rev., vol. 110, pp.4606-55. April 2010.

[6] J. Lee, O.K. Farha, J. Roberts, K.A. Scheidt, S.T. Nguyen and J.T. Hupp, " Metal-organic framework materials as catalysts, " Chem. Soc. Rev. , vol. 38, pp. 1450-1459, March 2009.

[7] J .Gascon, A .Corma , F .Kapteijn , F.X. Llabrés i Xamen, "Metal Organic Framework, Catalysis: Quo vadis?" *ACS Catal.*, vol. 4, pp: 361–378, January 2014.

[8] L. Ma and W. Lin, "Designing metal-organic frameworks for catalytic applications," Top Curr. Chem., vol. 293, pp.175-205, January 2010.

[9] K.S. Park, Z. Ni, A.P. Cote, J.Y. Choi, R. Huang, F.J. Uribe-Romo, H.K. Chae, M. O'Keeffe and O.M.Yaghi, " Exceptional chemical and thermal stability of zeolitic imidazolate frameworks, " Proc. Natl. Acad. Sci. U. S. A., vol. 103, pp. 10186-10191, June 2006.

[10] C.l. Chizallet, S. Lazare, D. Bazer-Bachi, F. Bonnier, V. Lecocq, E. Soyer, A-A. Quoineaud and N. Bats, "Catalysis of t ransesterification by a nonfunctionalized metal-organic framework: acido-basicity at the external surface of zif-8 probed by ftir and ab initio calculations," J. Am. Chem. Soc., vol. 132, pp. 12365–12377, September 2010.

[11] U.P.N. Tran, K.K.A. Le and N.T.S. Phan, "Expanding applications of metal−organic frameworks: zeolite imidazolate framework zif-8 as an efficient heterogeneous catalyst for the knoevenagel reaction, "ACS Catal.,vol. 1, pp.120-127, January 2011.

[12] J. Zakzeski, A. Dębczak, P.C.A. Bruijnincx and B.M. Weckhuysen, "Catalytic oxidation of aromatic oxygenates by the heterogeneous catalyst co-zif-9," Appl. Catal.,A., vol. 394, pp. 7 9-85, February 2011.

[13] L.T.L. Nguyen, K.K.A. Le, H.X and N.T.S. Phan, "Metal organic frameworks for catalysis: the knoevenagel reaction using zeolite imidazolate framework zif-9 as an efficient heterogeneous catalyst," Catal. Sci. Technol. vol. 2 , pp. 521-528, June 2012.

[14] C.M. Miralda, E.E. Macias, M. Zhu, P. Ratnasamy and M.A. Carreon, "Zeolitic imidazole framework-8 catalysts in the conversion of CO_2 to chloropropene carbonate," ACS Catal., vol. 2, pp. 180-183, December 2011.

[15] X. Zhou, H.P. Zhang, G.Y. Wang, Z.G. Yao, Y.R. Tang and S.S. Zheng, "Zeolitic imidazolate framework as efficient heterogeneous catalyst for the synthesis of ethyl methyl carbonate," J. Mol. Catal. *A:* Chem. Vol. *366*, pp.43-47, January 2013.

[16] A. Aijaz, Q. Xu, "Catalysis with metal nanoparticles immobilized within the pores of metal–organic frameworks," *J. Phys. Chem. Lett.* vol. *5*, pp.1400–1411, March 2014.

[17] Y-Q. Tian, Z-X. Chen, L-H. Weng, H-B. Guo, S. Gao and D.Y. Zhao, "Two polymorphs of cobalt(ii) imidazolate polymers synthesized solvothermally by using one organic template N,N-dimethylacetamide," Inorg Chem. , vol. 43, pp. 4631–4635, June 2004.

[18] R. Banerjee, A. Phan, B. Wang, C. Knobler, H. Furukawa, M. O'Keeffe and O.M. Yaghi, " High-throughput synthesis of zeolitic imidazolate frameworks and application to CO_2 capture," Science, vol. 319, pp. 939-943, February 2008.

[19] A.B.P. Lever, In.: Inorganic Electronic Spectroscopy, Elsevier, Amsterdam, 1968.

[20] L. Poul, N. Jouini and F. Fiévet, "Layered hydroxide metal acetates (metal = zinc, cobalt, and nickel): elaboration via hydrolysis in polyol medium and comparative study," Chem. Mater., vol. 12, pp. 3123-3132, September 2000.

21] A. Pande, K. Ganesan, A.K. Jain, P.K. Gupta and R.C. Malhotra, "A novel eco-friendly process for the synthesis of 2-chlorobenzylidenemalononitrile and its analogues using water as a solvent," Org. Process Res. Dev., vol. 9, pp. 133 -136, June 2005.

[22] J. Gascon, U. Aktay, M.D. Hernandez-Alonso, G.P.M. Van Klink, F. Kapteijn, (2009). "Amino-based metal-organic frameworks as stable, highly active basic catalysts," *J. Catal., vol.* 261, pp.75-87, Month 2009.

[23] F.X. Llabrés i Xamena, F.G. Cirujano, A. Corma, "An unexpected bifunctional acid base catalysis in IRMOF 3 for Knoevenagel condensation reactions," Micro and Meso Mat., vol.1, pp.1387-1811, March 2012.

[24] J. Hafizovic, M. Bjorgen, U. Olsbye, P.D.C. Dietzel, S. Bordiga, C. Prestipino, C. Lamberti, K.P. Lillerud, "The inconsistency in adsorption properties and powder xrd data of mof-5 is rationalized by framework interpenetration and the presence of organic and inorganic species in the nanocavities," J.Am.Chem. Soc., vol. 129, pp.3612–3620, Month 2007.

[24] J. Hafizovic, M. Bjorgen, U. Olsbye, P.D.C. Dietzel, S. Bordiga, C. Prestipino, C. Lamberti, K.P. Lillerud, "The inconsistency in adsorption properties and powder xrd data of mof-5 is rationalized by framework interpenetration and the presence of organic and inorganic species in the nanocavities," J.Am.Chem. Soc., vol. 129, pp.3612–3620, 2007.

[25] G. Calleja, J.A. Botas, M.G. Orcajo, M. Sánchez-Sánchez, "Differences between the isostructural IRMOF-1 and MOCP-L porous adsorbents," J.Porous Mater., vol. 17, pp.91-97, Feburary 2010.

[26] S. Neogi, M.K. Sharma, *P.K.* Bharadwaj, "Knoeven agel condensation and cyanosilylation reactions catalyzed by a MOF containing coordinatively unsaturated Zn(II) centers," *J. Mol. Catal. A: Chem., vol.299*, pp.*1*-4, Feburary 2009.

[27] N.T.S. Phan, C.W. Jones, "Highly accessible catalytic sites on recyclable organosilane functionalized magnetic nanoparticles: an alternative to functionalized porous silica catalysts," J. Mol. Catal. A: Chem., vol. 253, pp. 123-131, July 2006.

[28] K.M. Parida, S. Mallick, P.C. Sahoo and S.K. Rana, " A facile method for synthesis of amine-functionalized mesoporous zirconia and its catalytic evaluation in knoevenagel condensation," Appl. Catal.A., vol. 381, pp. 226-232, June 2010.

[29] X. Xin, X. Guo, H. Duan, Y. Li and H. Sun, "Efficient knoevenagel condensation catalyzed by cyclic guanidinium lactate ionic liquid as medium," Catal. Commun., vol. 8, pp.115-117, February 2007.

[30] S.S. Katkar, M.K, B.R. Arbad and S.B. Rathod, Indium "Modified mesoporous zeolite almcm-41 as a heterogeneous catalyst for the knoevenagel condensation reaction," Bull. Korean Chem. Soc., vol. 31, pp. 1301-1304, January 2010.

[31] S. Biella, G.L. Castiglioni, C. Fumagalli, L. Prati and M. Rossia, "Application of gold catalysts to selective liquid phase oxidation," Catal. Today, vol. 72, pp.43–49, 2002.

[32] H. Berndt, I. Pitsch, S. Evert, K. Struve, M.M. Pohl, J. Radnik and A. Martin, "Oxygen adsorption on au/al2o3 catalysts and relation to the catalytic oxidation of ethylene glycol to glycolic acid," Appl. Catal., A., vol. 244, pp. 169-179, 2003..

Supporting Appendix

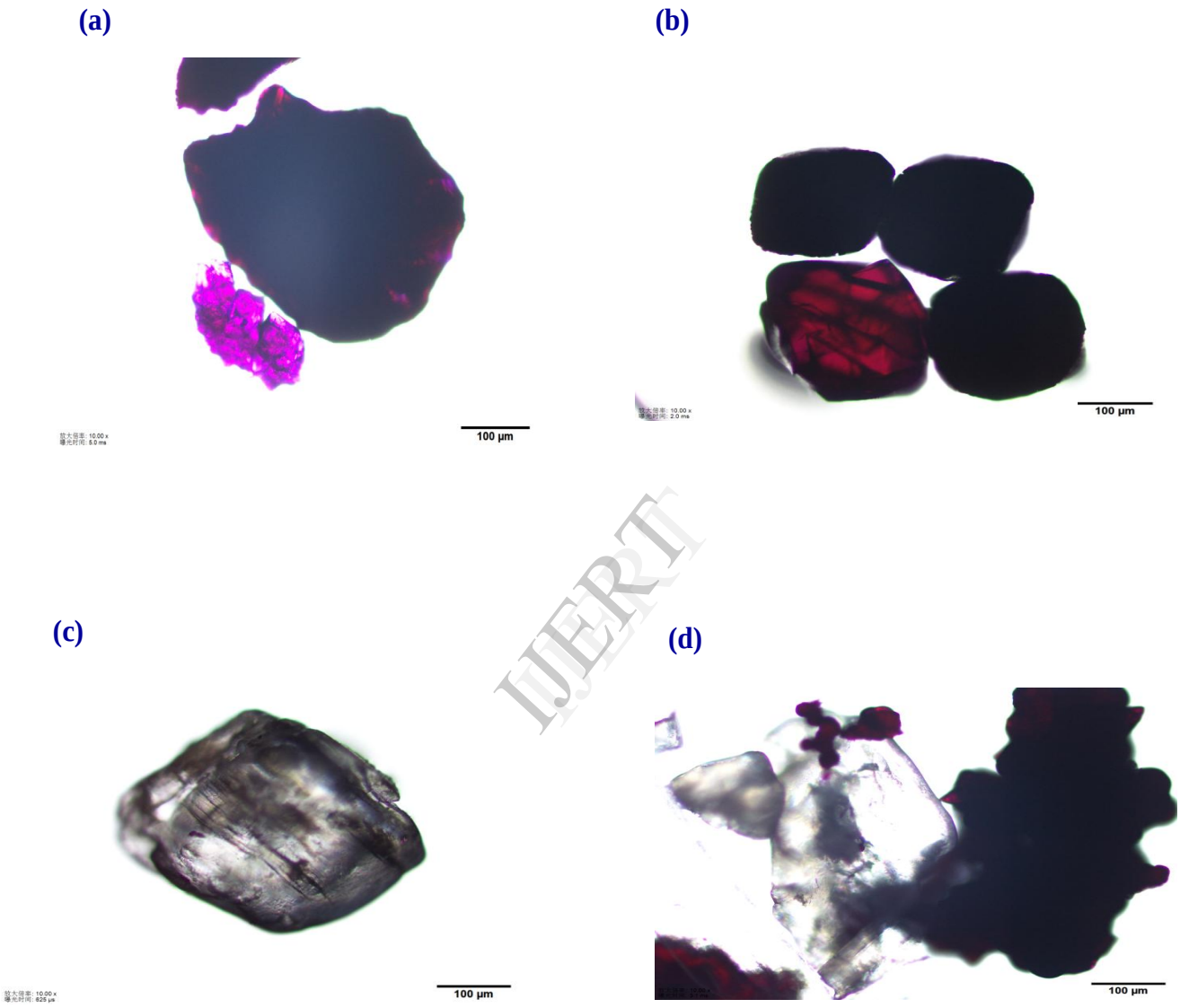

Fig. A. Optical micrograms of (a) $Co(im)_2 0.5DMA$; (b) $Co(im)_2 0.5DMF$ and (c-d) $Co(nim)_2$

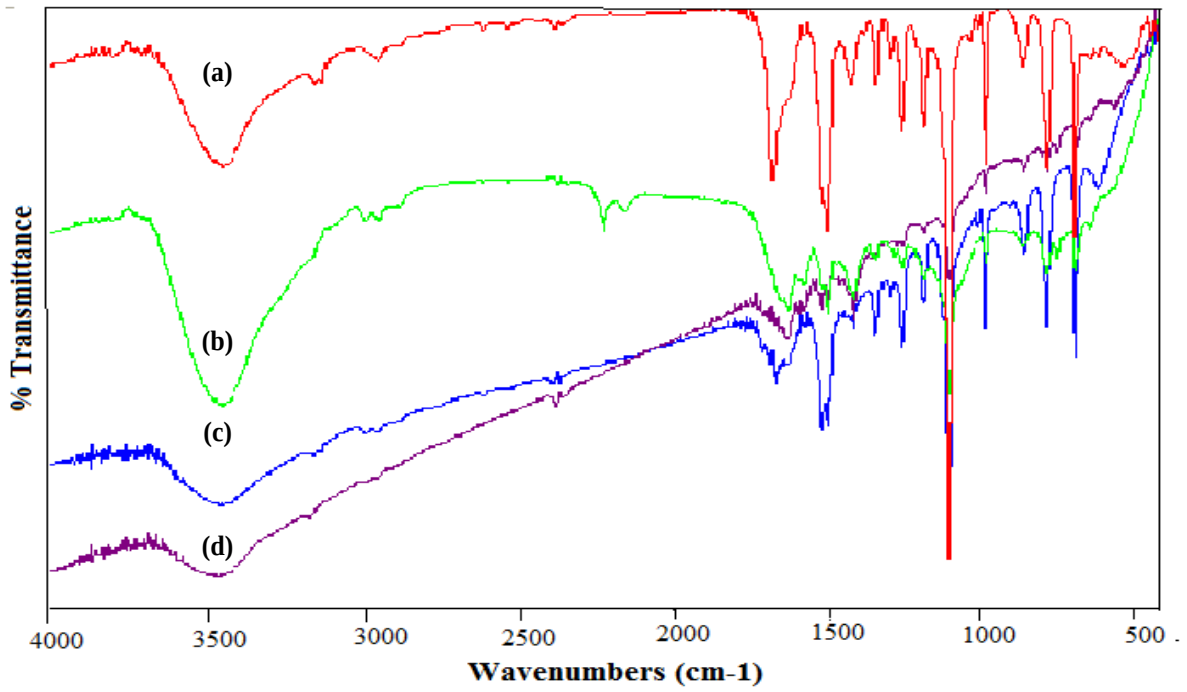

Fig. B1. FT-IR spectra of (a) fresh $Co(im)_2$0.5DMA ; after used for (b) Knoevenagel condensation (c) oxidation of ethybenzene and (d) ethylene glycol.

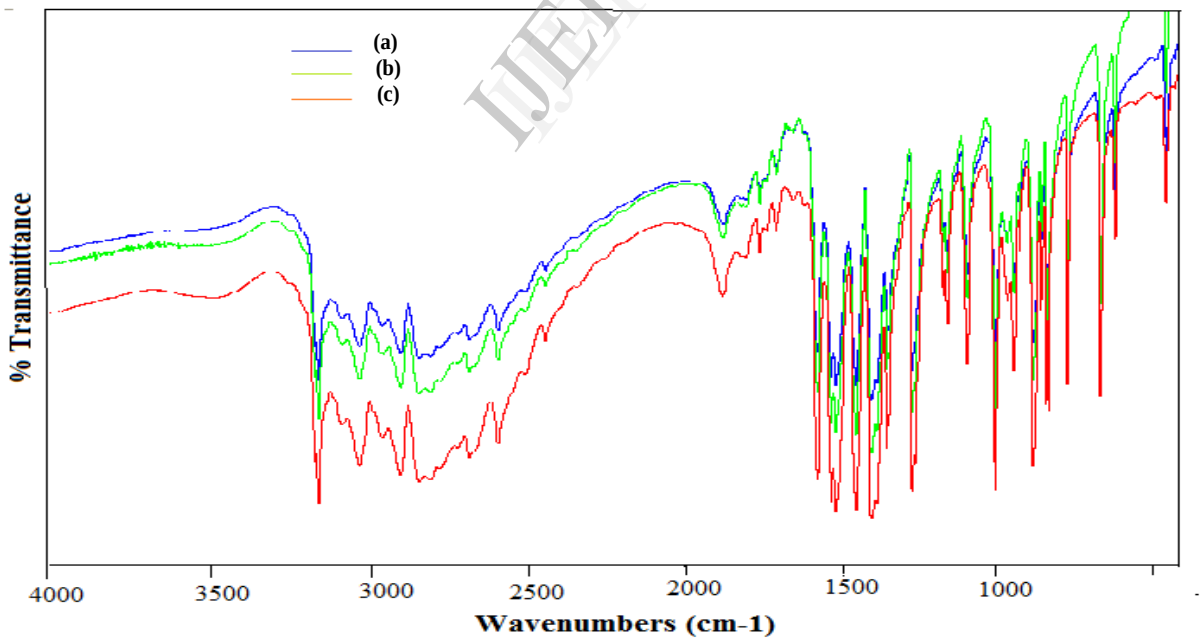

Fig.B2. FT-IR spectra of (a) $Co(nim)_2$; (b) after used as catalyst for Knoevenagel condensation; and (c) nitroimidazole.